

Quantum phase transition in the diopside magnetic lattice

CLAUDIUS GROS¹, PETER LEMMENS², K.-Y. CHOI³, G. GÜNTHERODT³, M. BAENITZ⁴
and H.H. OTTO⁵

¹ *Fachbereich Physik, Postfach 151150, Universität des Saarlandes, 66041 Saarbrücken, Germany*

² *IMNF, TU Braunschweig, D-38106 Braunschweig, Germany*

³ *II. Physikalisches Institut, RWTH-Aachen, Templergraben 55, 52056 Aachen, Germany*

⁴ *Max-Planck-Institut für Chemische Physik fester Stoffe, MPI-CPfS, D-01187 Dresden, Germany*

⁵ *Institut für Mineralogie und Mineralische Rohstoffe, TU Clausthal, D-38678 Clausthal-Zellerfeld, Germany*

PACS. 71.20.Be – Transition metals and alloys.

PACS. 73.43.Nq – Quantum phase transitions.

PACS. 75.10.Jm – Quantized spin models.

Abstract. – The study of quantum phase transitions [1], which are zero-temperature phase transitions between distinct states of matter, is of current interest in research since it allows for a description of low-temperature properties based on universal relations. Here we show that the crystal green diopside $\text{Cu}_6\text{Si}_6\text{O}_{18}\cdot 6\text{H}_2\text{O}$, known to the ancient Roman as the gem of Venus, has a magnetic crystal structure, formed by the Cu(II) ions, which allows for a quantum phase transition between an antiferromagnetically ordered state and a quantum spin liquid.

The gem-stone diopside $\text{Cu}_6\text{Si}_6\text{O}_{18}\cdot 6\text{H}_2\text{O}$ is a transparent green mineral build up from Si_6O_{18} single rings on a lattice, which sandwiches six-membered water rings down the (crystallographic) c -direction [2–4]. The magnetic Cu(II) ions are located between the Si_6O_{18} rings and form chiral chains along c , placed on an ab -honeycomb net and are there edge-sharing connected forming Cu(II) dimers.

We illustrate in fig. 1 the sublattice of the magnetic Cu(II)-ions. This three-dimensional magnetic lattice is characterized by only two coupling constants in between the spin-1/2 Cu(II)-moments. The magnetic sublattice is characterized by an antiferromagnetic intra-chain J_2 , which couples the Cu(II)-chains and an antiferromagnetic inter-chain coupling J_1 , leading for small J_1/J_2 to a AB-type Néel ordered state with doubling of the unit-cell along c . Alternatively one might consider the diopside magnetic lattice as made up by in-plane dimers of Cu(II)-ions, with an intra-dimer coupling strength of J_1 and an inter-dimer coupling along c of J_2 . For small J_2/J_1 a singlet-dimer state with a spin-gap and no long-range magnetic order is then realized.

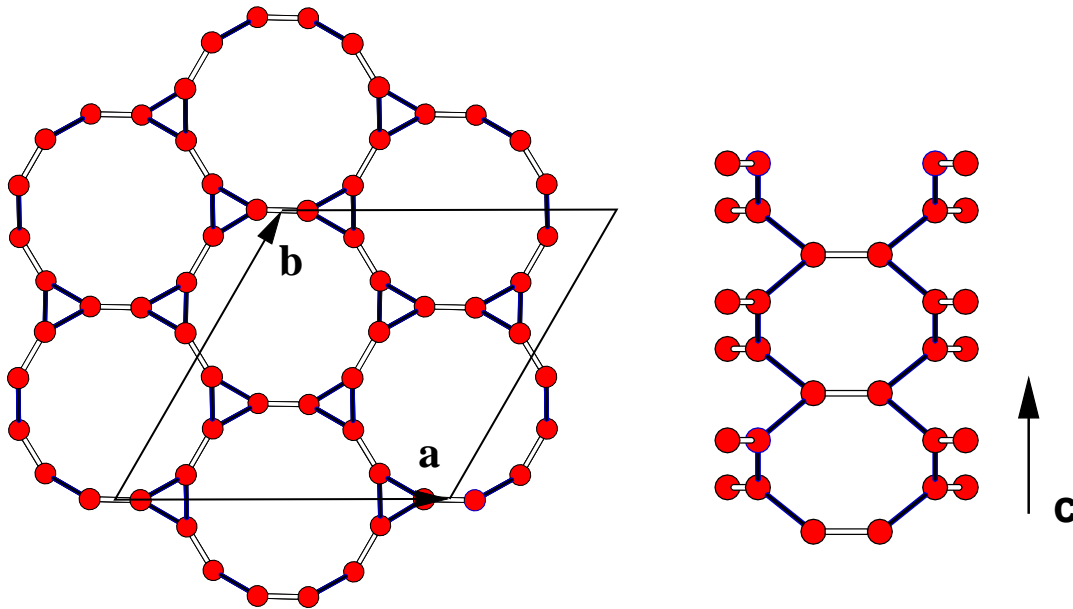


Fig. 1 – An illustration of Cu-sublattice of the diopside crystal structure. The rhombohedral unit-cell contains 18 equivalent Cu atoms arranged in six chains with three atoms down the c period. The inter/intra-chain magnetic coupling with strength J_1 and J_2 are indicated by white/black sticks. Left: An ab -plane. Not shown are the Si_6O_{18} rings, located inside the 12-membered Cu-rings. The rhombus denotes the in-plane hexagonal unit-cell. Right: two chiral chains along c .

In fig. 3 we present the phase-diagram of the diopside magnetic lattice, which we obtained from Quantum-Monte-Carlo (QMC) simulations, using the stochastic series expansion with worm-updates [5,6]. We used the parameterization $J_{1,2} = J(1 \pm \delta)$.

In order to determine the phase-diagram, an accurate estimate of the transition temperature to the ordered state is necessary. For this purpose we evaluated by QMC one of the Binder-cumulants [7], namely $\langle m_{AF}^2 \rangle / \langle |m_{AF}| \rangle^2$, where m_{AF} is the antiferromagnetic-order parameter (the staggered magnetization). The temperature at which the cumulants for different finite cluster intersect provide reliable estimates for the Neél temperature [7], see fig. 2. For the numerical simulations we used (n, n, m) clusters with periodic boundary conditions, where n^2 and m are the number of unit-cells in the ab -plane and along the c -axis respectively. We performed simulations for $(2, 2, 20)$, $(3, 3, 30)$ and $(4, 4, 40)$ clusters containing 1440, 4860 and 11520 Cu(II) sites respectively.

The linear raise of T_N in fig. 3 occurring for small inter-chain couplings J_1 is a consequence of the quantum-critical nature of the spin-1/2 Heisenberg chain realized for $J_1 = 0$. The magnetic correlation length $\xi(T)$ diverges as $\xi(T) \sim T^{-1}$ for a Heisenberg-chain at low-temperature. For small interchain couplings J_1 a chain-mean-field approach is valid [8] and the transition occurs when $J_2 \approx J_1 \xi(T_N) \sim J_1/T_N$. Consequently $T_N \sim T J_1/J_2$ for small J_1/J_2 .

The critical temperature for the transition, which is in the 3D-Heisenberg universality

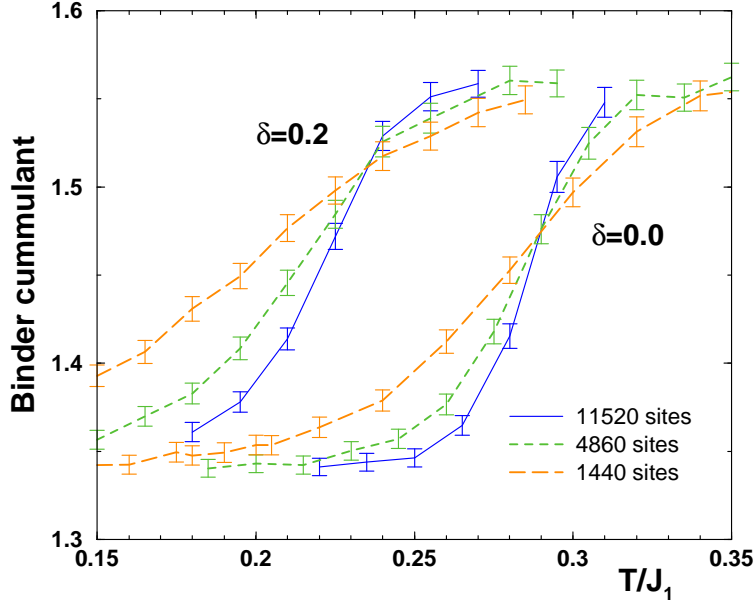


Fig. 2 – QMC-results for the dimensionless Binder-cumulant $\langle m_{AF}^2 \rangle / \langle |m_{AF}| \rangle^2$ for (nmn)-clusters with periodic boundary conditions. The lines are guides to the eye, the MC-estimates for the statistical errors are given. Shown are the results for $n = 2, m = 20$ (1440 sites), $n = 3, m = 30$ (4860 sites) and $n = 4, m = 40$ (11520 sites) and two value of δ ($J_{1,2} = J(1 \pm \delta)$).

class, is maximal for $\delta \approx -0.1$ and vanishes at a quantum critical point $\delta_c \approx 0.3$. Long-range magnetism is absent beyond this point and the ground-state is a quantum spin-liquid. For $J_2 = 0$ the diopside magnetic lattice decomposes into isolated dimers.

The magnitude of the singlet-triplet gap Δ in the spin-liquid state can be estimated by a fit of the low-temperature QMC-susceptibility to $\chi(T) \approx (k_B T / \Delta)^{d/2-1} e^{-\Delta / (k_B T)}$, where d is the dimensionality of the triplet-dispersion above the gap. For an isolated dimer $d = 0$, for a spin-ladder $d = 1$ [9]. This analysis would predict $d = 3$ for the diopside magnetic sublattice, but fits of the QMC-results for $\chi(T)$, presented in fig. 3, favor $d = 0$.

In fig. 4 we present the susceptibility of green diopside (using a crystal from Alтын Tyube, Kazakhstan) down the He-temperatures measured with a commercial SQUID magnetometer (Quantum Design). The data for magnetic field aligned parallel and perpendicular to the c -axis presented in the Inset of fig. 4 show clearly a transition to Néel-ordered stated at $T_N^{(exp)} = 15.5$ K. The moments are aligned along c for $T < T_N^{(exp)}$.

The QMC results for the susceptibility are to be compared, due to spin-rotational invariance, with the directional averaged of the experimental susceptibility, presented in the main panel of fig. 4. We have determined the Hamiltonian parameters $J_1 = J(1 + \delta)$ and $J_2 = J(1 - \delta)$ appropriate for diopside in the following way. For every $\delta < \delta_c$ the overall coupling constant J was determined by fixing the transition temperature to the experimental $T_N^{(exp)} = 15.5$ K. The spin-susceptibility in experimental units is then

$$\chi^{(exp)} = 0.375 * Z * (g^2 / J) * \Lambda_{mm} , \quad (1)$$

where $Z = 3$ is number of Cu^{2+} -ions in the primitive unit-cell. The dimensionless magnetization-fluctuation is $\Lambda_{mm} = (J\beta) (\langle m^2 \rangle - \langle m \rangle^2)$, where m is the magnetiza-

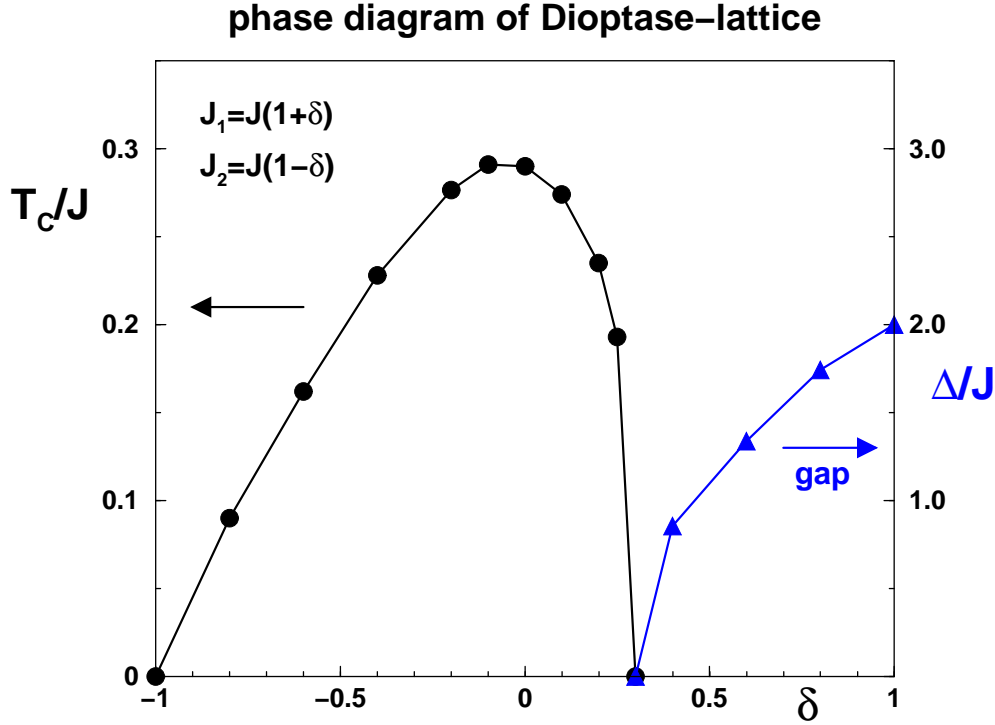


Fig. 3 – Phase diagram of the dioptase magnetic sublattice as obtained by Quantum Monte Carlo simulations. The lines are guides to the eye. The magnetic coupling constants are $J_{1,2} = J(1 \pm \delta)$ for inter/intra-chain couplings J_1/J_2 . At $\delta_c \approx 0.3$ a quantum phase transition occurs. The Neél temperature of the antiferromagnetically ordered phase for $\delta < \delta_c$ is given by the left y -axis. The antiferromagnetic order is of A-B type, with a doubling of the unit-cell along c . For $\delta > \delta_c$ a gap, given by the right y -axis, opens in the magnetic excitation spectrum and the state is a quantum spin-liquid.

tion. The g -factor was then determined, for every $\delta < \delta_c$, by adapting the right-hand-side of eq. 1 to the experimental susceptibility at high temperatures. The results are shown in fig. 4 together with the optimal values for J and g . We see that the optimal value $g \approx 2.1$ for the g -factor is relatively independent of δ .

We find two possible values for the ratio of the two-coupling (antiferromagnetic) constants J_1 and J_2 namely $\delta = 0.1$ and $\delta = -0.1$ which fit the experimental data equally well. Note that $\delta = -0.2$ does not agree well for $T < T_C^{(exp)}$. We attribute the residual discrepancies in between the theory and the experimental data to residual interactions, in addition to J_1 and J_2 .

It has been suggested previously [10] that the in-chain coupling J_2 might actually be ferromagnetic. We have studied therefore also the case for negative J_2 and found a quantum-phase-transition to a state with alternating ferromagnetic chains for $J_2 \approx -0.7 J_1$. We have performed the corresponding analysis to the one shown in fig. 4 for the case of ferromagnetic J_2 . We found very large deviations in between experiment and theory in this case, due to the fact that the susceptibility of ferromagnetic chains diverges for $T \rightarrow 0$.

To settle the ambiguity concerning the δ parameter we investigated the magnetic Raman

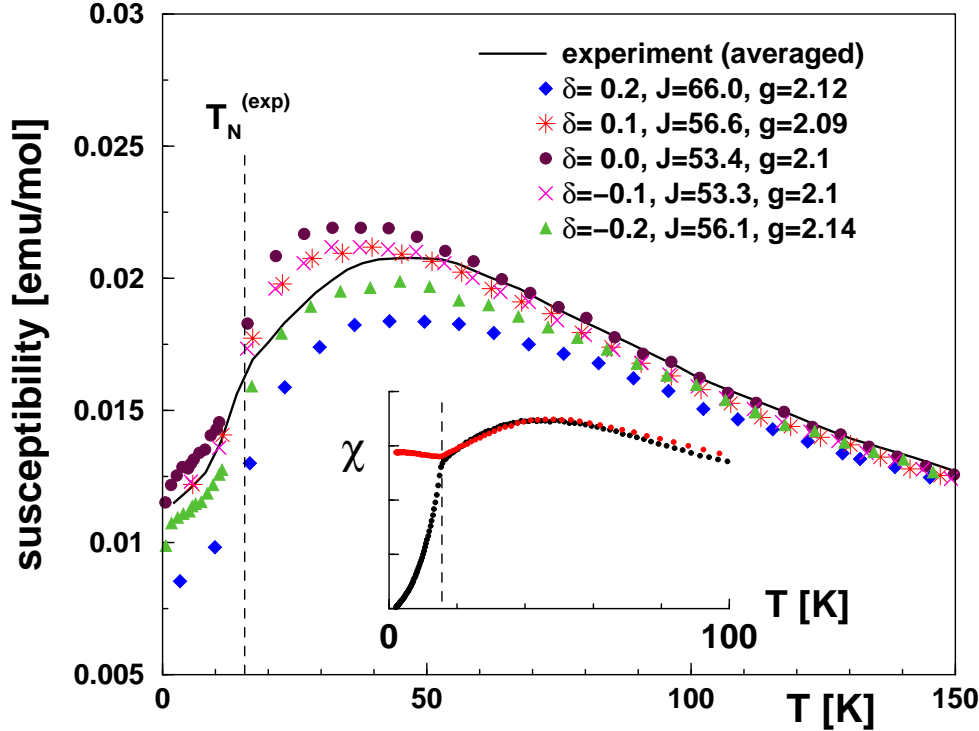


Fig. 4 – QMC-results for the susceptibility (in emu/mol) for various δ in comparison to the directional-averaged experimental susceptibility (solid line). Inset: The susceptibility χ for magnetic fields parallel/orthogonal to the c -axis (lower/upper) curve. The vertical dashed lines in the main panel and in the inset indicates the location of the Neél temperature.

spectrum of diopside as a function of temperature, as shown in fig. 5. The Raman scattering experiments were performed in quasi-backscattering geometry with a triple grating optical spectrometer (DILOR XY) with the $\lambda = 514$ nm laser line. Two modes at 48 and 85 cm^{-1} ($\equiv 69$ and 122 K) are magnetic as they exhibit a temperature dependence related to the transition. They show no anisotropy concerning the scattering selection rules. The excitation energies 69 K and 122 K correspond, for $\delta = +0.1$, to one and two inter-chain dimer excitation energy $J_1 = J(1+\delta)$, as expected for one- and two-magnon scattering processes. The lineshape of the magnetic two-magnon 122 K mode is very unusual, it is symmetric and not substantially broadened by either magnon-magnon scattering or density-of-states effects, in contrast to usual two-magnon scattering in normal 3D antiferromagnets [11]. This behavior indicates a very small dispersion of the underlying magnon branch. We consequently conclude that diopside is relatively close to a quantum-critical point.

In conclusion we have presented a novel magnetic lattice structure, the diopside magnetic lattice, which allows for a quantum-phase transition. This lattice is realized in green diopside $\text{Cu}_6\text{Si}_6\text{O}_{18} \cdot 6\text{H}_2\text{O}$ and in the recently synthesized isostructural germanate $\text{Cu}_6\text{Ge}_6\text{O}_{18} \cdot 6\text{H}_2\text{O}$ [12,13], a promising candidate to study further aspect of the phase diagram presented in detail fig. 3.

We acknowledge fruitful discussions with Matthias Troyer on the stochastic series expansion and Felicien Capraro for data analysis.

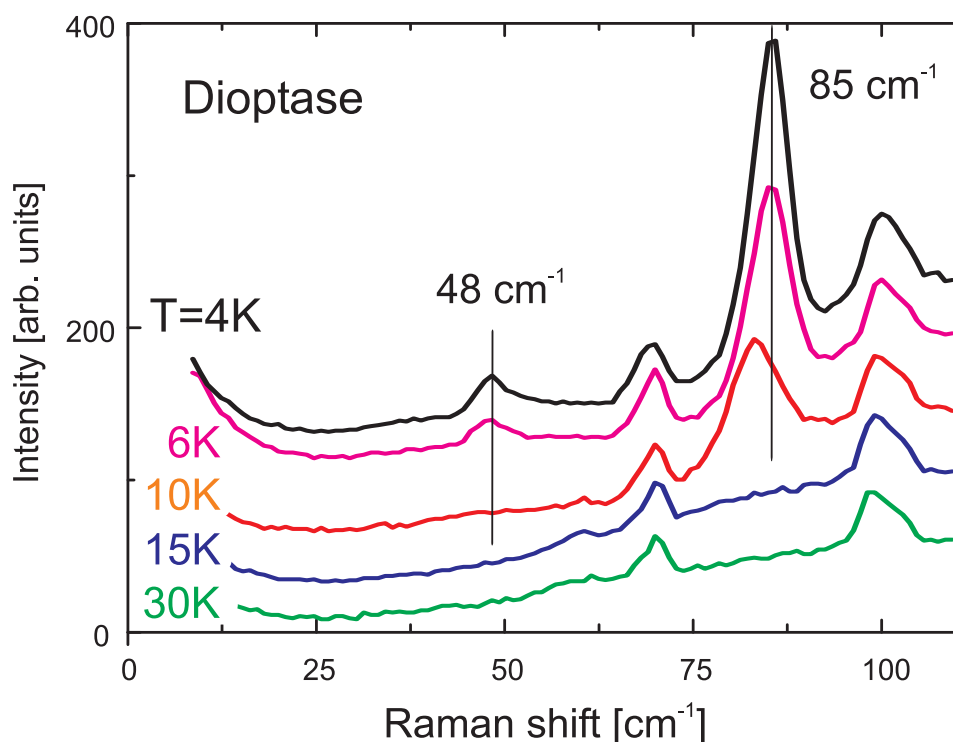


Fig. 5 – Low energy Raman spectrum of diophtase in xx-polarization. The modes at 48 and 85 cm^{-1} (\equiv 69 and 122 K) show a strong increase of intensity for $T < T_N = 15.5$ K and correspond to one- and two-magnon processes. The temperature independent modes at 70 and 100 cm^{-1} are phonons.

REFERENCES

- [1] S. Sachdev, *Cambridge University Press*, Cambridge, 1999.
- [2] H.G. Heide, K. Boll-Dornberger, E. Thilo and E.M. Thilo, *Acta Cryst.* **8**, 425-430 (1955).
- [3] P.H. Ribbe, G.V. Gibbs and M.M.A. Hamil, *Amer. Mineral.* **62**, 807-811 (1977),
- [4] N.V. Belov, B.A. Maksimov, Z. Nozik Yu and L.A. Muradyan, *Soviet Phys. - Doklady* **23** 215-217 (1978).
- [5] A.W. Sandvik and J. Kurkijärvi, *Phys. Rev. B* **43**, 5950-5961 (1991).
- [6] A.W. Sandvik, *Phys. Rev. B* **59**, R14 157-R14160 (1999).
- [7] K. Binder, *Rep. Prog. Phys.* **60**, 487-559 (1997).
- [8] H.J. Schulz, *Phys. Rev. Lett.* **77**, 2790-2793 (1996).
- [9] D.C. Johnston, R.K. Kremer, M. Troyer, X. Wang, A. Klumper, S.L. Bud'ko, A.F. Panchula and P.C. Canfield, *Phys. Rev. B* **61**, 9558-9606 (2000).
- [10] M. Wintenberger, G. André and W.F. Gardette, structure of black diophtase. *Solid State Comm.* **87**, 309-317 (1993).
- [11] P.A. Fleury and H.J. Guggenheim, *Phys. Rev. Lett.* **24**, 1346 (1970).
- [12] H.-J. Brandt and H.H. Otto, *Z. Kristallogr.* **212**, 34 (1997).
- [13] M. Baenitz, M. Dischner, H.H. Otto, F. Steglich and H. Wolfram, *Z. Kristallogr. Suppl.* **17**, 167 (2001).